JACC: CARDIOVASCULAR IMAGING VOL. 2, NO. 12, 2009

ISSN 1936-878X/09/$36.00
PUBLISHED BY ELSEVIER INC. DOI:10.1016/j.jcmg.2009.07.012

Quantifying the Role of Regional Dyssynchrony on Global Left Ventricular Performance

Bouchra Lamia, MD, MPH, PhD,* Masaki Tanabe, MD,† Hyung Kook Kim, MD,*
Lauren Johnson, PhD,‡ John Gorcsan III, MD,† Michael R. Pinsky, MD*†
Pittsburgh, Pennsylvania

OBJECTIVES We hypothesize that left ventricular (LV) segmental dyssynchrony, quantified by paradoxical systolic wall thinning, determines changes in global LV performance in a model of canine right ventricular (RV) pacing-induced dyssynchrony and the response to cardiac resynchronization therapy (CRT).

BACKGROUND Quantification of LV dyssynchrony is important to assess the impact of CRT.

METHODS Seven pentobarbital-anesthetized open-chest dogs had LV pressure-volume relations and mid-LV short-axis echocardiographic speckle tracking radial strain imaging during right atrial (RA) pacing, RV pacing to simulate left bundle branch block, and CRT using RV pacing plus either LV free-wall (CRTfw) and apical (CRTa) pacing. The area under the segmental LV time-radial strain positive and negative curves defined global thickening and thinning, respectively. Dyssynchrony was defined as the maximum time difference between earliest and latest peak segmental positive strain among 6 radial sites.

RESULTS RA pacing had minimal dyssynchrony (58 $\pm$ 40 ms). RV pacing induced both dyssynchrony (213 $\pm$ 67 ms, $p < 0.05$) and reduced LV stroke work (SW) (67 $\pm$ 51 mJ, $p < 0.05$). CRTfw and CRTa decreased dyssynchrony (116 $\pm$ 47 ms and 50 $\pm$ 34 ms, respectively, $p < 0.05$ vs. RV pacing), but only CRTa restored LV SW to RA pacing levels. RV pacing decreased global thickening (129 $\pm$ 87% $\cdot$ ms) compared with RA pacing (258 $\pm$ 133% $\cdot$ ms, $p < 0.05$), whereas CRTfw and CRTa restored regional thickening to RA pacing levels (194 $\pm$ 83% $\cdot$ ms and 230 $\pm$ 76% $\cdot$ ms, respectively). The sum of thickening and thinning during RV (230 $\pm$ 88% $\cdot$ ms vs. 258 $\pm$ 133% $\cdot$ ms, $p < 0.05$) correlated ($r = 0.98$) with RA thickening, suggesting that all the loss of LV function was due to thinning.

CONCLUSIONS Dyssynchrony causes proportional changes in regional LV wall thinning and global LV SW that were reversed by CRT, suggesting that dyssynchrony impairs LV systolic function by causing paradoxical regional wall thinning and that CRT effectiveness can be monitored by its reversal. Thus, monitoring paradoxical regional thinning reversal may be used to define CRT effectiveness. (J Am Coll Cardiol Img 2009;2:1350–6) © 2009 by the American College of Cardiology Foundation

From the *Department of Critical Care Medicine, University of Pittsburgh Medical Center, Pittsburgh, Pennsylvania; and the †Cardiovascular Institute and ‡Cardiovascular Systems Laboratory, Department of Bioengineering, University of Pittsburgh, Pittsburgh, Pennsylvania. This study was supported in part by NIH awards HL04503, HL067181, and HL073198.

Manuscript received May 7, 2009; revised manuscript received July 23, 2009, accepted July 28, 2009.

Quantification of left ventricular (LV) dyssynchrony by echocardiography is important for the assessment of baseline cardiac performance and to quantify cardiac resynchronization therapy (CRT) effectiveness (1–14). However, the quantitative contribution that regional dyssynchrony and its reversal during CRT make toward global LV contraction effectiveness is unclear.

Tissue Doppler strain analysis can be applied for evaluation of ischemia, LV and right ventricular (RV) function, and mechanical dyssynchrony (1,3,6,8,12,13,15). However, visualization of tissue Doppler phase shift analysis requires a minimal angle of incidence to measure tissue velocity. Thus, these studies are usually restricted to assessment of longitudinal LV movement, greatly limiting its ability to assess global LV motion. Speckle tracking of B-mode gray-scale 2-dimensional (2D) echocardiographic images does not require specific angles of incidence of the myocardium relative to the echo sensor. These speckle-tracking techniques have been validated against sonomicrometry in vivo and cardiac magnetic resonance (CMR) in vitro (16–18). Recent data using CMR have shown that circumferential strain is more sensitive to assess cardiac dyssynchrony than longitudinal motion (19,20). Furthermore, we documented that regional radial strain analysis can quantify ventricular dyssynchrony using both tissue Doppler radial strain (21–23) and speckle-tracking radial strain in humans (24). In this study, we hypothesized that LV segmental dyssynchrony, quantified by paradoxical systolic wall thinning, determines changes in global LV performance during dyssynchrony and the response to CRT. To assess LV systolic wall thickening and thinning, we used echocardiographic speckle-tracking techniques to quantify regional strain and its impact on global LV performance in our intact acute canine model (21,23).

METHODS

Preparation. Seven mongrel dogs, weighing 21.0 ± 1.5 kg were studied after an overnight fast. The protocol was approved by the institutional animal care and use committee and conformed to the American Heart Association position on research animal use. All dogs were anesthetized with sodium pentobarbital (30 mg/kg induction; 1.0 mg/kg/h with intermittent boluses, as needed) and mechanically ventilated. A 6-F 11-pole multielectrode conductance catheter (Webster Laboratories, Irvine, California) and a LV micromanometer catheter (MPC-500, Millar, Houston, Texas) were placed for LV pressure-volume analysis, as previously described (21). After a median sternotomy, a snare occluder was placed around the inferior vena cava to transiently alter preload. The pericardium was opened and epicardial pacing wires (A & E Medical Corp., Farmingdale, New Jersey) were placed on the right atrium (RA), RV free-wall near the anterior infundibulum, LV mid-free wall near the mid-posterior-lateral wall, and LV apex for multisite stimulation. The pericardium was reopposed and positive end-expiratory pressure (PEEP) applied to re-expand the lungs. Afterward, 5 cm H_2O PEEP was applied for the remainder of the experiment. Fluid resuscitation was performed prior to starting the protocol to restore apneic LV end-diastolic volume to pre-sternotomy values.

Hemodynamic data analysis. LV pressure, volume, and electrocardiogram signals were digitized at 150 Hz and stored on disk for offline analysis. LV peak systolic pressure, stroke volume (SV), and stroke work (SW) were used to assess global LV performance. SW was calculated as the integral of the pressure-volume loop.

Echocardiography. An echocardiographic system (Aplio SSA-770A, Toshiba Medical Systems Corp., Tokyo, Japan) was used to obtain images with a 3.0 MHz transducer directly applied to the heart. Digital B-mode grayscale 2D and tissue Doppler cine loops from 3 consecutives beats were obtained at end-expiratory apnea from mid-LV short-axis view at depths of 8 cm using a fixed transducer position. Mid-LV short-axis views were selected with the papillary muscle as a consistent internal anatomic landmark, and great care was taken to orient the image to the most circular geometry possible. The temporal resolution of the tissue Doppler system was frame rates of 49 Hz with a pulse repetition frequency of 4.5 kHz. The precise spatial resolution of the speckle-tracking algorithm was estimated to be in the range of 0.5 to 1 mm. Gain settings were adjusted for echo imaging to optimize endocardial definition. Offline analysis of radial strain was then performed on digitally stored images (ApliQ, Toshiba Medical Systems Corp.).

Speckle-tracking strain analysis. The speckle-tracking analysis was used to generate regional LV

ABBREVIATIONS AND ACRONYMS

CMR = cardiac magnetic resonance

CRT = cardiac resynchronization therapy

CRTa = cardiac resynchronization therapy using right ventricular and apical pacing

CRTfw = cardiac resynchronization therapy using right ventricular and left ventricular free-wall pacing

LV = left ventricular

RA = right atrium

RV = right ventricular

SV = stroke volume

SW = stroke work

strain (25,26) from echocardiographic images. Strain-time waveforms were generated for frame-by-frame movement of stable patterns of natural acoustic markers present in ultrasound tissue images over the cardiac cycle as previously described by our group (24). Briefly, a circular region of interest was traced on the endocardial and epicardial border of the mid-LV short-axis view. Speckles within the region of interest were tracked in subsequent frames by the imaging software. The location shift of these speckles from frame to frame, representing tissue movement, provided the spatial and temporal data. Myocardial thickening/thinning was calculated as change in length/initial length between specific endocardial and epicardial speckles (ΔL/Lo). Myocardial thickening was represented as positive strain, color-coded yellow; and thinning was represented as negative strain, color-coded blue, and superimposed on conventional 2D images. The software divides the short-axis image into 6 equal segments. Thickening and thinning values from multiple circumferential points were calculated and data averaged into 6 segmental time-strain curves, as previously validated in humans (24) and dogs (27).

Thickening and thinning were quantified by speckle tracking at the same 6 regions of interest during RA pacing as heart rate control, RV pacing, cardiac resynchronization therapy using right ventricular and left ventricular free-wall pacing (CRTfw), and cardiac resynchronization therapy using right ventricular and left ventricular apex pacing (CRTa), as previously described in this model (23). Time to peak strain from each of 6 time-strain curves was determined with dyssynchrony defined as the difference

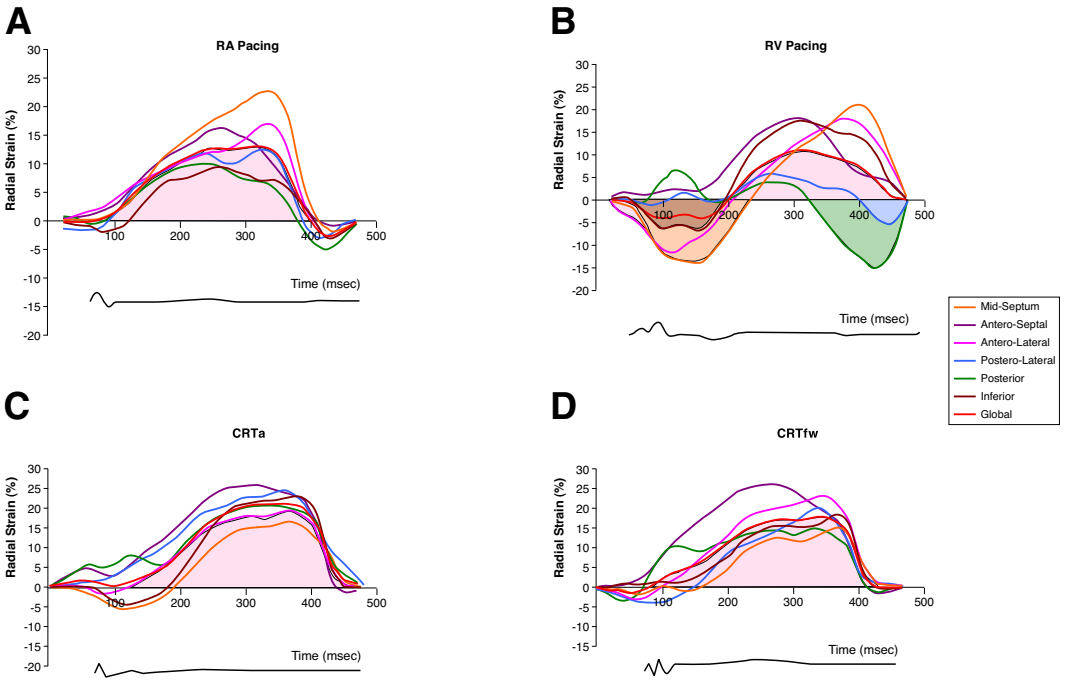

Figure 1. Regional Radial Time-Strain Activity Curves

(A) Right atrial (RA) pacing (normal). Example of radial time-strain curves from 6 segments of left ventricular short-axis view using speckle tracking and global systolic wall thickening during RA pacing. The global systolic wall thickening was calculated as the area under the curve (AUC) of the global positive strain **(pink)**. **(B)** RA-right ventricular (RV) pacing (left bundle branch block–like contraction). Example of radial time-strain curves from 6 segments of left ventricular short-axis view using speckle tracking and global systolic wall thickening during RV pacing. The global systolic wall thickening was calculated as the AUC of the global positive strain **(pink)**. The global systolic wall thinning was calculated as the sum of AUCs of individual segments systolic thinning. In this example, these areas of systolic thinning are color coded for the inferior segment **(brown)**, posterior segment **(green)**, posterolateral segment **(blue)**, anterolateral segment **(pink)**, and the mid-septum segment **(orange)**. RV pacing decreased global thickening and increased global thinning compared with RA pacing. **(C)** Cardiac resynchronization therapy using right ventricular and apical pacing (CRTa). Example of radial time-strain curves from 6 segments of left ventricular short-axis view using speckle tracking and global systolic wall thickening during CRTa. CRTa restored systolic wall thickening compared with right ventricular pacing. **(D)** Cardiac resynchronization therapy using right ventricular and left ventricular free-wall pacing (CRTfw). Example of radial time-strain curves from 6 segments of left ventricular short-axis view using speckle tracking and global systolic wall thickening during CRTfw. CRTfw restored systolic wall thickening compared with right ventricular pacing.

between earliest and latest segments (21). Global radial strain was calculated as averaged radial strain from 6 segments. Peak global strain was used as a marker of global contractility. Global thickening was calculated as the area under the curve of the global positive strain. RA pacing served as baseline control, whereas RV pacing served as maximal dyssynchrony. We calculated the thinning as the sum of areas under the curves of negative individual segment strains (Fig. 1B). Global performance was quantified as LV SW. We assumed that if the observed reduction in global performance was explained by regional dyssynchrony, then thickening would be associated with LV SW, and the sum of thickening plus thinning during RV pacing should be correlated to thickening during RA pacing.

Protocol. All measurements were made during apnea with 5 cm H_2O PEEP. RA pacing was performed at frequencies 5 to 10 min^{-1} above the intrinsic rhythm. RA pacing was defined as normal ventricular contraction. All succeeding ventricular pacing studies were done with sequential pacing at an atrio-ventricular delay of 30 ms, preventing atrial fusion beats but also eliminating atrial augmentation of LV filling. High RV free-wall pacing was used to induce a left bundle branch block (LBBB)-like contraction pattern. We then compared the impact of CRTfw and CRTa on regional and global LV performance. The order of CRTfw and CRTa was alternated among animals. Pacing was maintained for >30 s before measurements were made. In practice, hemodynamic stability usually took <15 s to occur. Between each ventricular-paced rhythm, animals were returned to RA pacing and all hemodynamic variables allowed to stabilize before the next step was initiated. Three heart cycles were analyzed per pacing mode.

Statistical analysis. Data are expressed as mean ± SD. Repeated measures of analysis of variance were used for comparisons among different pacing modalities. A paired sample Student *t* test was used for the statistical comparison of parametric values. These paired *t* tests are made without correction for multiple comparisons. Since RV pacing, CRTa, and CRTfw did not have atrial contribution to diastolic filling, LV end-diastolic volume was lower than in RA pacing. Thus, global LV performance comparisons were made only between RV pacing, CRTa, and CRTfw. Significance was determined as $p < 0.05$. Interobserver variability was assessed in 10 randomly selected studies for segmental time to peak strain and global peak strain, and was calculated as the ratio (%) of the difference between the values obtained by each observer (expressed as absolute value) divided by the mean of the 2 values. Intraobserver variability was calculated by a similar approach.

RESULTS

Effects of pacing on global LV function. RV pacing decreased LV SV and SW compared with RA pacing. Whereas CRTa significantly improved LV SV and SW, CRTfw did not alter either LV SV or SW (Table 1, Fig. 2).

Radial strain dyssynchrony. The maximum time difference from earliest to latest peak strain among 6 segments was minimal with RA pacing (58 ± 40 ms). RV pacing displayed early septal thickening and opposing free-wall thinning, typically seen in human LBBB (25). Maximal time-strain difference increased during RV pacing (213 ± 67 ms, $p < 0.05$ vs. RA pacing) (Table 1, Fig. 3), whereas both CRTa and CRTfw reduced maximal time difference (50 ± 34 ms

Table 1. Alterations in LV Hemodynamic Characteristics, Radial Dyssynchrony, and Systolic Thickening During the 4 Pacing Modes

	RA Pacing	RV Pacing	CRTa	CRTfw
HR, beats/min	131 ± 15	131 ± 15	131 ± 15	131 ± 15
LVP_{Peak}, mm Hg	96 ± 20	76 ± 19	79 ± 22	79 ± 22
EDV, ml	46 ± 19	41 ± 18*	39 ± 19	39 ± 18
SV, ml	15 ± 5	11 ± 3*	16 ± 4†	12 ± 4
SW, mJ	140 ± 60	67 ± 51*	117 ± 40†	77 ± 36
dP/dt_{max}, mm Hg · s^{-1}	351 ± 386	1,025 ± 313	1,109 ± 306	1,144 ± 321
dP/dt_{min}, mm Hg · s^{-1}	−1,639 ± 550	−1,084 ± 453	−1,228 ± 497	−1,209 ± 529
EDP, mm Hg	12 ± 7	11 ± 6	11 ± 6	10 ± 6
Dyssynchrony, ms	58 ± 40	213 ± 67*	50 ± 34†	116 ± 47†
Thickening, % · ms	258 ± 133	129 ± 87*	230 ± 76†	194 ± 83†

*$p < 0.05$ RA pacing versus RV pacing, †$p < 0.05$ CRTa or CRTfw versus RV pacing.
CRTa = cardiac resynchronization therapy using right ventricular and apical pacing; CRTfw = cardiac resynchronization therapy using right ventricular and free-wall pacing; dP/dt_{max} = maximum rate of change of left ventricular pressure; dP/dt_{min} = minimum rate of change of left ventricular pressure; EDP = end-diastolic pressure; EDV = end-diastolic volume; HR = heart rate; LV = left ventricular; LVP_{Peak} = left ventricular peak pressure; RA = right atrial; RV = right ventricular; SV = stroke volume; SW = stroke work.

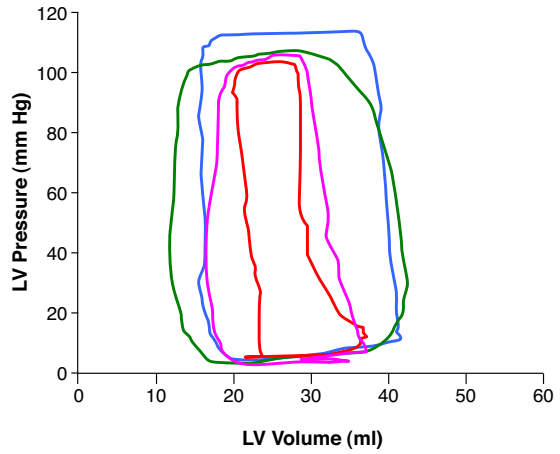

Figure 2. LV Pressure-Volume Loops for the 4 Study Conditions

LV pressure-volume loops during RA **(blue line)**, RV **(red line)**, CRTa **(green line)**, and CRTfw **(pink line)** for the same animal as Figure 1. Note that stroke volume and stroke work decreased during RV pacing and were restored during CRTa. LV = left ventricular; other abbreviations as in Figure 1.

and 116 ± 47 ms, CRTa and CRTfw, respectively, $p < 0.05$ vs. RV pacing) (Fig. 3). RV pacing resulted in less LV wall thickening (258 ± 133% · ms vs. 129 ± 87% · ms, $p < 0.05$), whereas both CRTa and CRTfw restored thickening to RA pacing levels (230 ± 76% · ms and 194 ± 83% · ms, CRTa and CRTfw, respectively, $p < 0.05$ vs. RV pacing).

Systolic thinning during RV pacing occurred for 101 ± 41% · ms. The sum of thickening and thinning during RV pacing correlated with thickening during RA pacing (230 ± 88% · ms and 258 ± 133% · ms, respectively, $p < 0.05$, $r = 0.98$), suggesting that all the LV function loss was due to thinning.

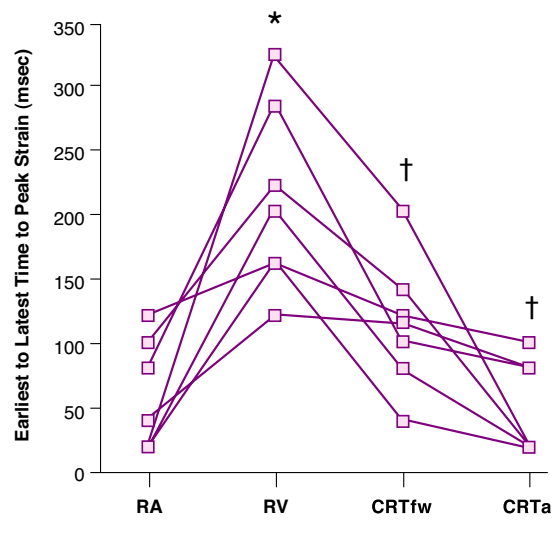

Figure 3. Individual Earliest to Latest Time to Peak Strain Across Pacing Modes

Individual values of earliest to latest peak segmental strain using speckle tracking from RA pacing, RV pacing, CRTfw, and CRTa. *$p < 0.05$ RA pacing versus RV pacing, †$p < 0.05$ CRTa or CRTfw versus RV pacing. Abbreviations as in Figure 1.

Effects of radial dyssynchrony on global LV function. Global radial strain, defined as the average among 6 radial segments, decreased during RV pacing compared to RA pacing (22 ± 9% vs. 13 ± 8%, $p < 0.05$) and was restored during both CRTa and CRTfw (22 ± 6% and 19 ±7%, respectively, $p < 0.05$ vs. RV pacing).

Reproducibility. Intraobserver and interobserver variability for segmental time to peak strain expressed as the mean percent error (absolute difference/mean) was 4 ± 8% and 4 ± 8%, respectively (n = 56 segments), and for global peak strain was 13 ± 9% and 15 ± 9%, respectively (n = 10 studies).

DISCUSSION

RV pacing-induced dyssynchrony caused decrements in global LV function and regional contraction, as quantified by global hemodynamics and regional strain. Both CRTa and CRTfw reduced LV dyssynchrony, but only CRTa improved both regional and global LV function relative to RV pacing. Thus, regional contraction abnormalities, as quantified by paradoxical systolic wall thinning, parallel impaired global LV performance during pacing-induced dyssynchrony but only partially explain the effects of CRT from different resynchronization sites on global LV performance. Importantly, regional dyssynchrony as assessed by segmental thickening relative to thinning of a mid-axis cross-sectional image varies in proportion with global LV function during RA and RV pacing. Because our model allowed us to compare normal contraction with dyssynchronous contraction, a luxury not available under clinical conditions of CRT, we documented that the combined thickening and thinning of RV pacing equaled the normal thickening time of RA pacing, suggesting that dyssynchrony-associated global LV impairment can be quantified by the relative degree of systolic thinning. CRTa and CRTfw resulted in similar improvements in thickening compared with RV pacing but different quantitative effects of global LV performance. Thus, factors other than mid-plane radial contraction such as torsion and longitudinal strain analysis may be needed to determine the subsequent improvement in global LV performance during CRT.

These observations have clinical relevance. Radial thickening plays a major role in LV ejection. Myocardial contraction not only shortens cardiac myocytes, it

thickens them. Our data suggest that the changes in global LV performance can be quantified by dyssynchronous strain activity because contraction dyssynchrony across the entire myocardium can be used as quantitative markers of dyssynchrony and LV global performance. Speckle tracking assesses strain in a nondirectional fashion, unlike tissue Doppler imaging, allowing one to analyze isolated regional thinning and the timing of peak thickening during systole across the entire myocardium. Although CMR analysis of contraction dyssynchrony is powerful in assessing the impact of regional contraction dyssynchrony on global performance (28), its data acquisition is cumbersome and its post-acquisition data analysis laborious.

Our data agree with previous studies showing that dyssynchronous contraction increases radial strain differences across LV segments when assessed by M-mode, tissue Doppler imaging, and CMR scanning (11,19,22,28). We recently demonstrated that speckle-tracking radial strain can quantify dyssynchrony and predict immediate and long-term responses to CRT in humans (24).

Our findings that LV global and regional functions are differentially affected by pacing site agree with previous investigators (21,23,29). LV function was better if the CRT pacing was from the LV apex. These data agree with our previous study (21) and those of others (19). Presumably, apical pacing activates the intact His-Purkinje system before it travels from the LV apex upwards toward the base. We previously showed that patients in whom LV lead position was concordant with the site of latest mechanical activation by speckle-tracking radial strain had a greater increase in ejection fraction from baseline than patients with discordant lead position (24). Furthermore, a time-to-peak strain difference in humans between septal to free-wall peak cutoff value of >130 ms identified those candidates who would improve LV function following CRT (24). All our animals except 1 had a pacing-induced dyssynchrony >130 ms and improved their performance with CRT. In the 1 who did not, neither CRTa nor CRTfw improved synchrony. These data support the hypothesis that CRT can only improve performance if baseline dyssynchrony is above some minimum threshold.

Study limitations. There are 2 major limitations of this study. First, we studied an intact canine model without intrinsic conduction defects or impaired contractility. We (23), and others (29), have documented that LV apical CRT is superior to LV free-wall CRT in terms of global LV performance and resynchronization in a model of pacing-induced dyssynchrony. However, similar apical pacing superiority has not been reported in human CRT studies. Dyssynchrony usually occurs through structural myocardial defects, which themselves are not similarly distributed across all CRT candidates. Our data demonstrate, however, that different pacing site CRT may have differing effects on global LV performance. Second, speckle-tracking echocardiography is dependent on frame rates, as well as image resolution. Low acquisition frame rates degrade assessment of regional myocardial motion and its subsequent strain rate analysis. In contrast, increasing the frame rate reduces scan-line density, which reduces image resolution (25,26). Suffoletto et al. (24) found frame rates in the range of 30 to 90 Hz with a mean of 65 Hz suitable for speckle-tracking analysis. Accordingly, in our study we used a mean frame rate of 49 Hz suitable for speckle tracking analysis.

Acknowledgments

The authors thank Lisa Gordon and Don Severyn for their expert technical assistance.

Reprint requests and correspondence: Dr. Michael R. Pinsky, University of Pittsburgh, Critical Care Medicine, 606 Scaife Hall, 3550 Terrace Street, Pittsburgh, Pennsylvania 15261. *E-mail: pinskymr@upmc.edu.*

REFERENCES

1. Armstrong G, Pasquet A, Fukamachi K, Cardon L, Olstad B, Marwick T. Use of peak systolic strain as an index of regional left ventricular function: comparison with tissue Doppler velocity during dobutamine stress and myocardial ischemia. J Am Soc Echocardiogr 2000;13:731–7.
2. Bax JJ, Bleeker GB, Marwick TH, et al. Left ventricular dyssynchrony predicts response and prognosis after cardiac resynchronization therapy. J Am Coll Cardiol 2004;44:1834–40.
3. Edvardsen T, Skulstad H, Aakhus S, Urheim S, Ihlen H. Regional myocardial systolic function during acute myocardial ischemia assessed by strain Doppler echocardiography. J Am Coll Cardiol 2001;37:726–30.
4. Gorcsan J 3rd, Kanzaki H, Bazaz R, Dohi K, Schwartzman D. Usefulness of echocardiographic tissue synchronization imaging to predict acute response to cardiac resynchronization therapy. Am J Cardiol 2004;93:1178–81.
5. Grines CL, Bashore TM, Boudoulas H, Olson A, Shafer P, Wooley CF. Functional abnormalities in isolated left bundle branch block: the effect of interventricular asynchrony. Circulation 1989;79:845–53.
6. Kanzaki H, Bazaz R, Schwartzman D, Dohi K, Sade LE, Gorcsan J 3rd. A mechanism for immediate reduction in mitral regurgitation after cardiac resynchronization therapy: insights from mechanical activation strain mapping. J Am Coll Cardiol 2004;44:1619–25.
7. Kass DA, Chen CH, Curry C, et al. Improved left ventricular mechanics from acute VDD pacing in patients with dilated cardiomyopathy and ventricular conduction delay. Circulation 1999;99:1567–73.

8. Pellerin D, Sharma R, Elliott P, Veyrat C. Tissue Doppler, strain, and strain rate echocardiography for the assessment of left and right systolic ventricular function. Heart 2003;89: Suppl 3:iii9–17.
9. Penicka M, Bartunek J, De Bruyne B, et al. Improvement of left ventricular function after cardiac resynchronization therapy is predicted by tissue Doppler imaging echocardiography. Circulation 2004;109: 978–83.
10. Pitzalis MV, Iacoviello M, Romito R, et al. Ventricular asynchrony predicts a better outcome in patients with chronic heart failure receiving cardiac resynchronization therapy. J Am Coll Cardiol 2005;45:65–9.
11. Pitzalis MV, Iacoviello M, Romito R, et al. Cardiac resynchronization therapy tailored by echocardiographic evaluation of ventricular asynchrony. J Am Coll Cardiol 2002;40:1615–22.
12. Sutherland GR, Di Salvo G, Claus P, D'Hooge J, Bijnens B. Strain and strain rate imaging: a new clinical approach to quantifying regional myocardial function. J Am Soc Echocardiogr 2004;17:788–802.
13. Urheim S, Edvardsen T, Torp H, Angelsen B, Smiseth OA. Myocardial strain by Doppler echocardiography. Validation of a new method to quantify regional myocardial function. Circulation 2000;102:1158–64.
14. Yu CM, Fung WH, Zhang Q, et al. Tissue Doppler imaging is superior to strain rate imaging and post-systolic shortening on the prediction of reverse remodeling in both ischemic and non-ischemic heart failure after cardiac resynchronization therapy. Circulation 2004;110:66–73.
15. Sade LE, Kanzaki H, Severyn DA, Dohi K, Gorcsan J. Quantification of radial mechanical dyssynchrony in patients with left bundle branch block and idiopathic dilated cardiomyopathy without conduction delay by tissue displacement imaging. Am J Cardiol 2004;94:514–8.
16. Amundsen BH, Helle-Valle T, Edvardsen T, et al. Noninvasive myocardial strain measurement by speckle tracking echocardiography: validation against sonomicrometry and tagged magnetic resonance imaging. J Am Coll Cardiol 2006;47:789–93.
17. Langeland S, D'Hooge J, Wouters PF, et al. Experimental validation of a new ultrasound method for the simultaneous assessment of radial and longitudinal myocardial deformation independent of insonation angle. Circulation 2005;112:2157–62.
18. Toyoda T, Baba H, Akasaka T, et al. Assessment of regional myocardial strain by a novel automated tracking system from digital image files. J Am Soc Echocardiogr 2004;17:1234–8.
19. Helm RH, Leclercq C, Faris OP, et al. Cardiac dyssynchrony analysis using circumferential versus longitudinal strain: implications for assessing cardiac resynchronization. Circulation 2005;111:2760–7.
20. Reant P, Labrousse L, Lafitte S, et al. Experimental validation of circumferential, longitudinal, and radial 2-dimensional strain during dobutamine stress echocardiography in ischemic conditions. J Am Coll Cardiol 2008;51: 149–58.
21. Dohi K, Pinsky MR, Kanzaki H, Severyn D, Gorcsan J 3rd. Effects of radial left ventricular dyssynchrony on cardiac performance using quantitative tissue Doppler radial strain imaging. J Am Soc Echocardiogr 2006;19: 475–82.
22. Dohi K, Suffoletto MS, Schwartzman D, Ganz L, Pinsky MR, Gorcsan J 3rd. Utility of echocardiographic radial strain imaging to quantify left ventricular dyssynchrony and predict acute response to cardiac resynchronization therapy. Am J Cardiol 2005;96: 112–6.
23. Johnson L, Kim HK, Tanabe M, et al. Differential effects of left ventricular pacing sites in a canine model of contraction dyssynchrony. Am J Physiol Heart Circ Physiol 2007;293: H3046–55.
24. Suffoletto MS, Dohi K, Cannesson M, Saba S, Gorcsan J 3rd. Novel speckle-tracking radial strain from routine black-and-white echocardiographic images to quantify dyssynchrony and predict response to cardiac resynchronization therapy. Circulation 2006;113:960–8.
25. Leitman M, Lysyansky P, Sidenko S, et al. Two-dimensional strain-a novel software for real-time quantitative echocardiographic assessment of myocardial function. J Am Soc Echocardiogr 2004;17:1021–9.
26. Reisner SA, Lysyansky P, Agmon Y, Mutlak D, Lessick J, Friedman Z. Global longitudinal strain: a novel index of left ventricular systolic function. J Am Soc Echocardiogr 2004;17: 630–3.
27. Tanabe M, Lamia B, Tanaka H, Schwartzman D, Pinsky MR, Gorcsan J. Echocardiographic speckle tracking radial strain imaging to assess ventricular dyssynchrony in a pacing model of resynchronization therapy. J Am Soc Echocardiogr 2008;21: 1382–8.
28. Kapetanakis S, Kearney MT, Siva A, Gall N, Cooklin M, Monaghan MJ. Real-time three-dimensional echocardiography: a novel technique to quantify global left ventricular mechanical dyssynchrony. Circulation 2005;112: 992–1000.
29. Peschar M, de Swart H, Michels KJ, Reneman RS, Prinzen FW. Left ventricular septal and apex pacing for optimal pump function in canine hearts. J Am Coll Cardiol 2003;41: 1218–26.

Key Words: canine model ■ cardiac resynchronization therapy ■ dyssynchrony ■ echocardiography ■ speckle tracking ■ ventricular performance.